



Universitat Politècnica De Catalunya, Barcelona-Tech.
Masters in Computational Mechanics

Course
Computational Solid Mechanics

Assignment 1

'Continuum Damage Models'

By

KIMEY K. WAZARE

Introduction:

Continuum Damage Mechanics is used to model material which are characterized by loss of stiffness. It proposes the continuum mechanics theory to identify or represent defects at microscopic level.

Solution:

A) Rate Independent Model

1. The Continuum Isotropic Damage Models:

a) Non-symmetric Damage Model –

In this damage model (Granular materials), tensile and compressive elastic limits are different. For this model, algorithm is defined, for the ratio of uniaxial elastic limit compression to tensile strength. Figure 1, justifies that the elastic limit of the elastic domain is different for tensile and compression.

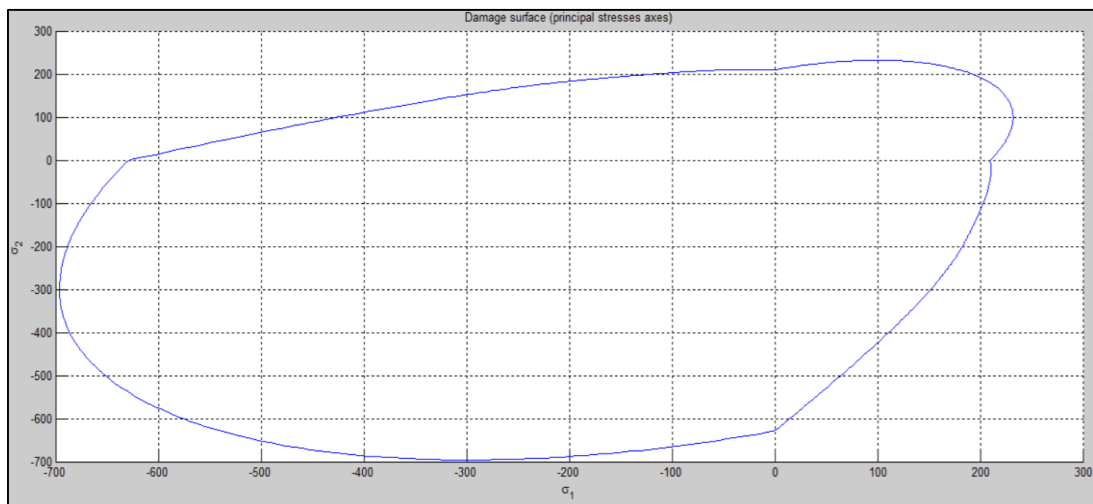


Fig 1: Damage Surface for Non-Symmetric Damage Model

b) Tensile Damage Model–

This damage model fails only to tension. Compression can't be reached as it is infinity because when principal stresses are negative elastic limit is beyond imagination. For this model, algorithm is defined and Figure 2, justifies that when all the principal stresses are positive.

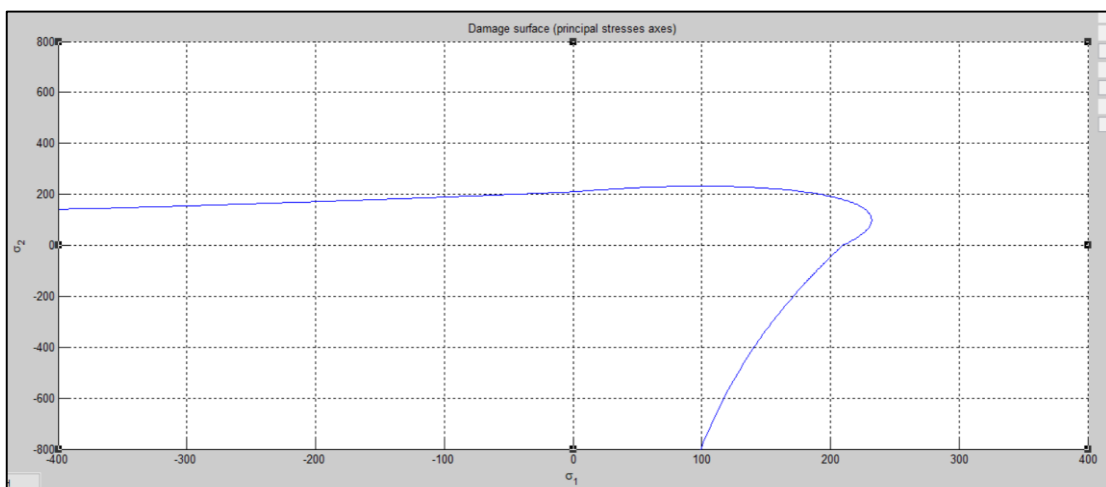


Fig: Damage Surface for Tensile Damage Model

2. Exponential Hardening/Softening –

An exponential hardening/softening model has been implemented choosing $q_{\infty} = 10 - 6 * r_0$. It can never be negative. It is implemented, when $r \rightarrow \infty, q \rightarrow q_{\infty}$. In the case of hardening the $q_{\infty} > r_0$, and for the case of softening $q_{\infty} < r_0$.

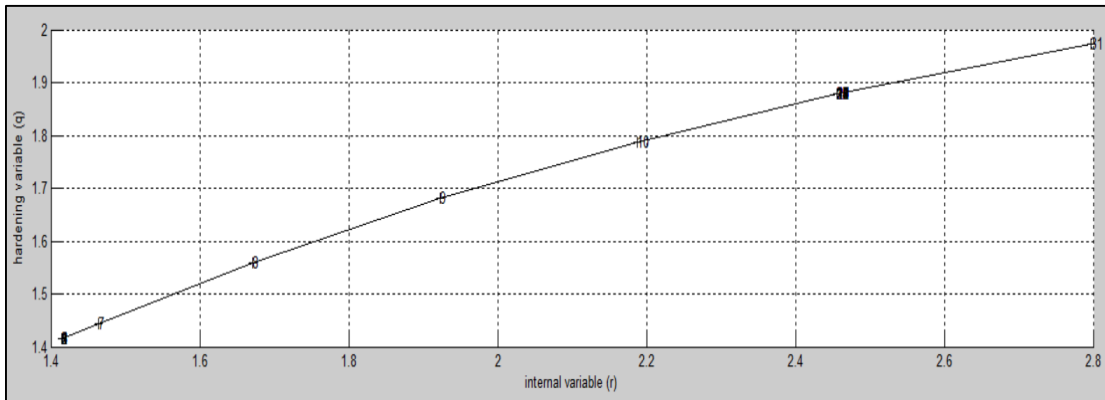


Fig 3: Variation between Internal Variable & Hardening Variable

3. Implementing the models.

Case 1. $(\Delta\sigma I(1) = \alpha, \Delta\sigma Z = 0), (\Delta\sigma I(1) = -\beta, \Delta\sigma Z = 0), (\Delta\sigma I(1) = \gamma, \Delta\sigma Z = 0)$

1.1 Non-Symmetric Damage Model:

$(\Delta\sigma I(1) = 400, \Delta\sigma Z = 0), (\Delta\sigma I(1) = -1200, \Delta\sigma Z = 0), (\Delta\sigma I(1) = 300, \Delta\sigma Z = 0)$

Initially, the effective and actual stresses are same till it reaches elastic domain. The uniaxial elastic tensile load occurs; the actual stress path becomes straight line till it reaches origin. Fig 4 shows evolution of damage surface and physical occurrence of loading & unloading.

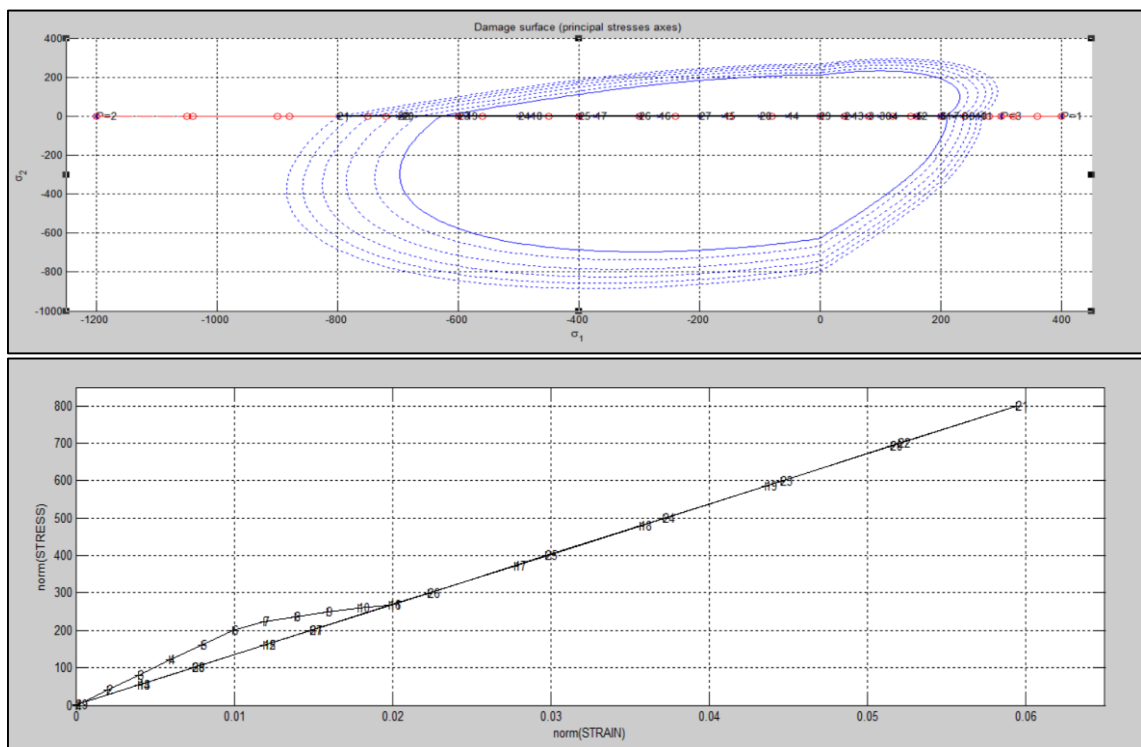


Fig 4: Stress Space & Stress-Strain Curve for the Non-Symmetric model

1.2 Tensile only Damage Model

$$(\Delta\sigma_I(1) = 400, \Delta\sigma_Z = 0), (\Delta\sigma_I(1) = -1200, \Delta\sigma_Z = 0), (\Delta\sigma_I(1) = 300, \Delta\sigma_Z = 0)$$

Initially, the effective and actual stresses are same till it reaches elastic domain. The elastic limit in the compression can't be reached. The uniaxial elastic tensile load occurs; the actual stress path becomes straight line till it reaches origin. Fig 5 shows evolution of damage surface and physical occurrence of loading & unloading.

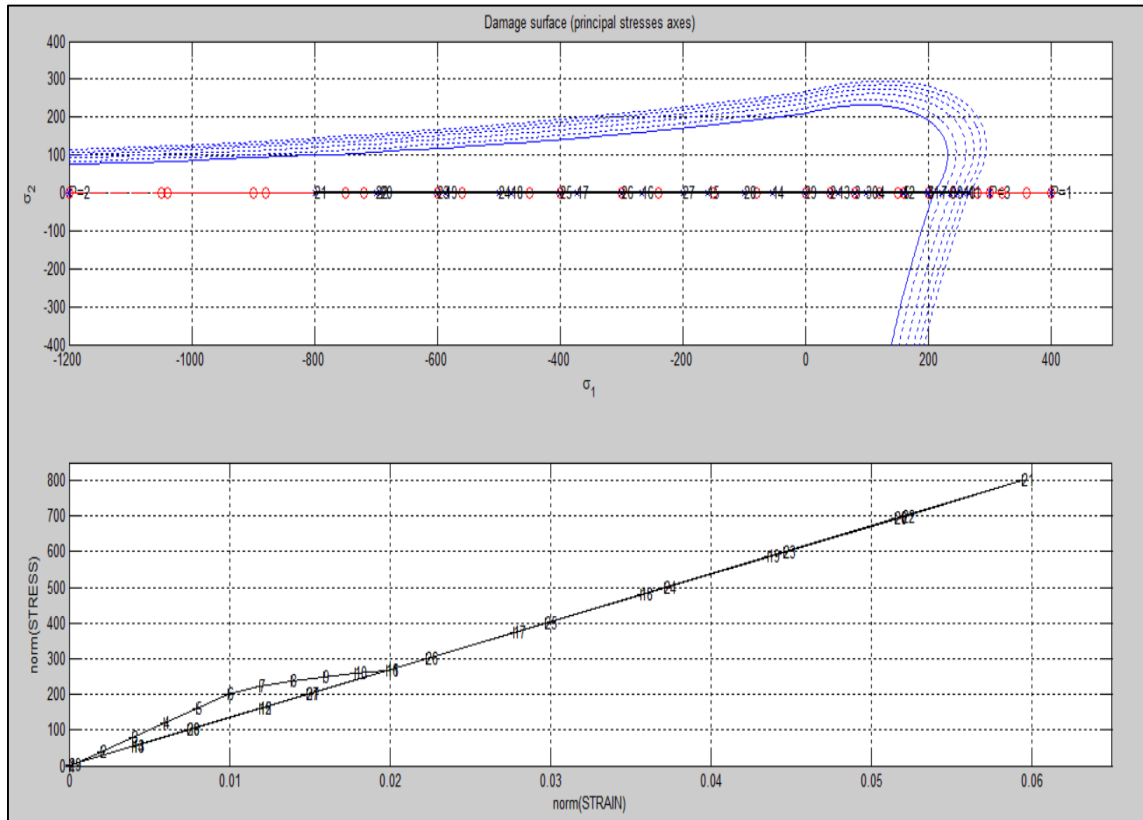


Fig 5: Stress Space & Stress-Strain Curve for the Tensile Damage model

Case 2. $(\Delta\sigma_I(1) = \alpha, \Delta\sigma_Z = 0), (\Delta\sigma_I(1) = -\beta, \Delta\sigma_Z = -\beta), (\Delta\sigma_I(1) = \gamma, \Delta\sigma_Z =)$

2.1 Non-Symmetric Damage Model

$$(\Delta\sigma_I(1) = 150, \Delta\sigma_Z = 0), (\Delta\sigma_I(1) = -1200, \Delta\sigma_Z = -1200), (\Delta\sigma_I(1) = 700, \Delta\sigma_Z = 700)$$

Initially, the effective and actual stresses are same till it reaches elastic domain for uniaxial. When the stress path leaves the elastic domain for tension, loading appears ($d > 0$). After that when biaxial tensile unloading/compressive loading occurs. After which, when the stress path leaves the elastic limit of compression, loading occurs. Fig 6 shows evolution of damage surface and physical occurrence of loading & unloading.

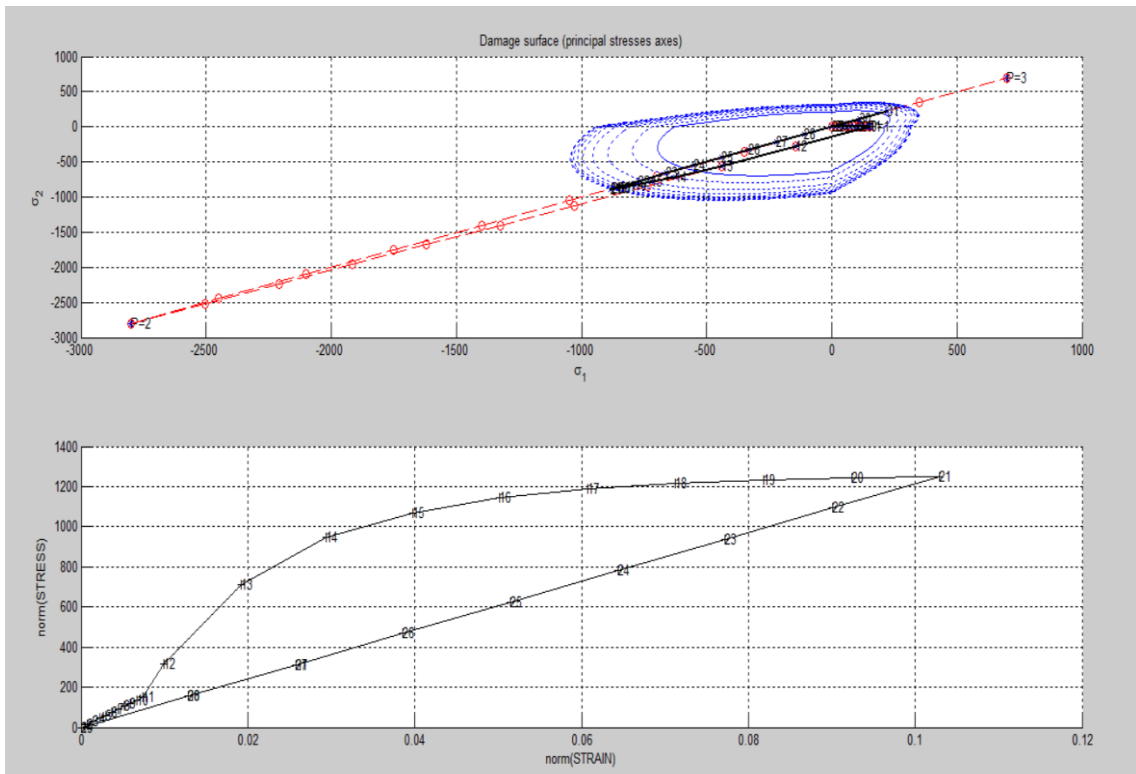


Fig 6: Stress Space & Stress-Strain Curve for the Non Symmetric model

2.2 Tensile only Damage Model

$(\Delta\sigma_I(1) = 200, \Delta\sigma_Z = 0), (\Delta\sigma_I(1) = -1700, \Delta\sigma_Z = -1700), (\Delta\sigma_I(1) = 300, \Delta\sigma_Z = 300)$

Initially, the effective and actual stresses are same till it reaches elastic domain for uniaxial. In this biaxial tensile unloading/ compressive loading occurs but compressive never occurs. Fig 7. shows evolution of damage surface and physical occurrence of loading & unloading.

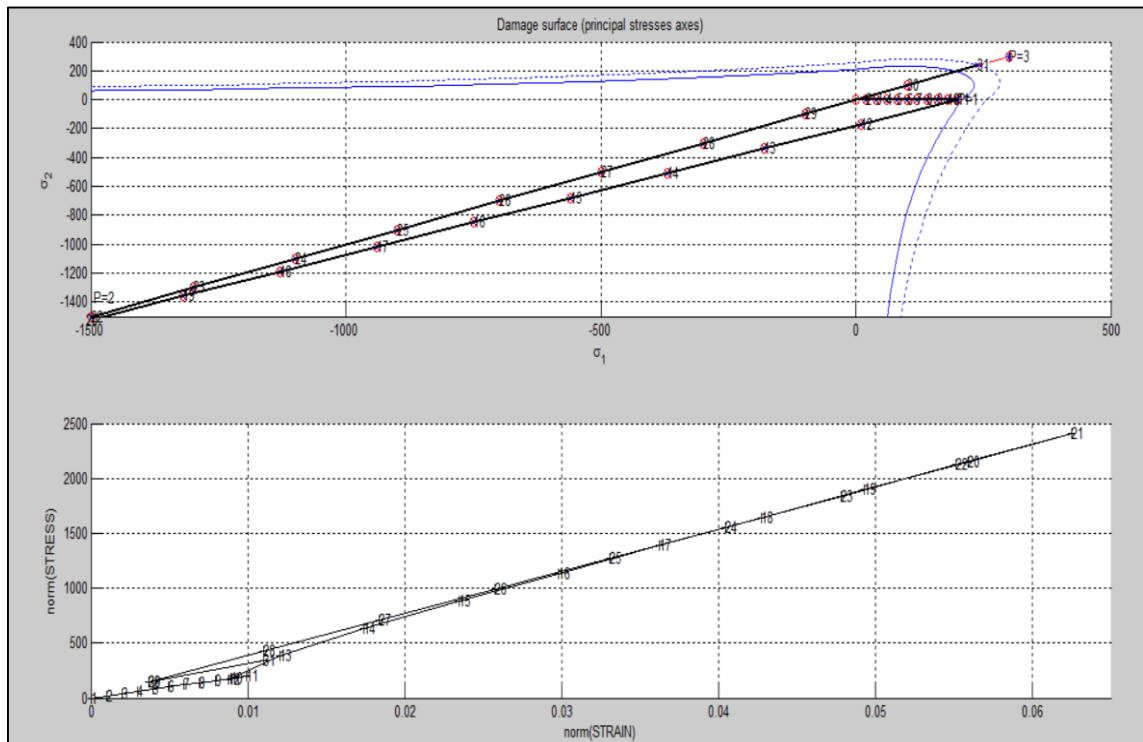


Fig 7: Stress Space & Stress-Strain Curve for the Tensile Damage model

Case 3. $(\Delta\sigma_I(1) = \alpha, \Delta\sigma_Z = \alpha), (\Delta\sigma_I(1) = -\beta, \Delta\sigma_Z = -\beta), (\Delta\sigma_I(1) = \gamma, \Delta\sigma_Z = \gamma)$

3.1 Non-Symmetric Damage Model:

$(\Delta\sigma_I(1) = 1200, \Delta\sigma_Z = 1200), (\Delta\sigma_I(1) = -1800, \Delta\sigma_Z = -1800), (\Delta\sigma_I(1) = 600, \Delta\sigma_Z = 600)$

Initially, the effective and actual stresses are same till it reaches elastic domain for biaxial. In this biaxial tensile unloading/ compressive loading occurs. Fig 8. shows evolution of damage surface and physical occurrence of loading & unloading.

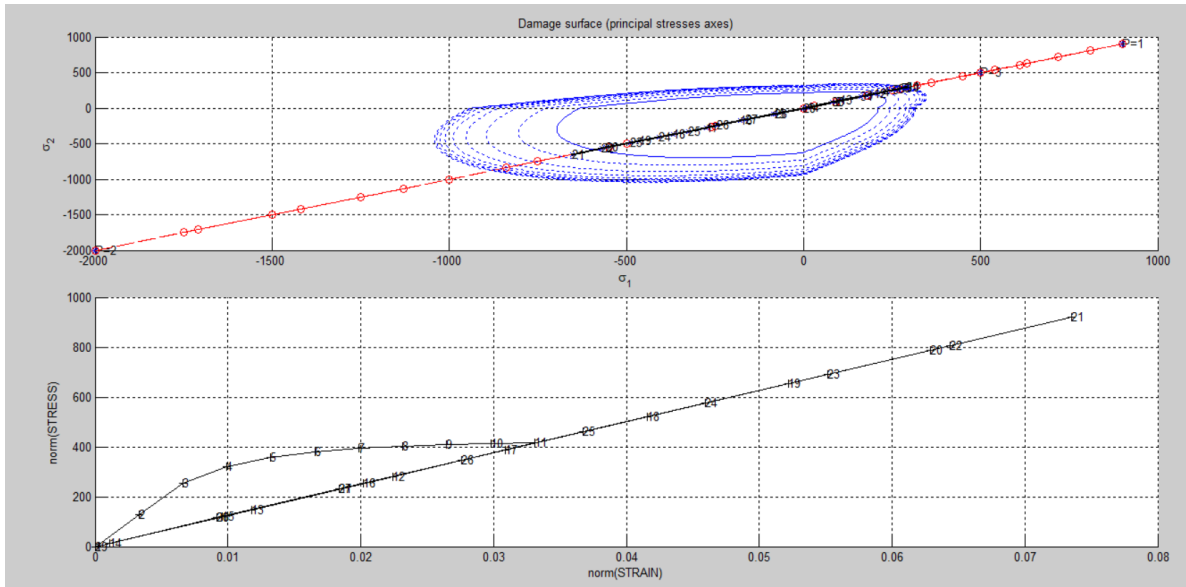


Fig 8: Stress Space & Stress-Strain Curve for the Non Symmetric model

3.2 Tensile only Damage Model:

$(\Delta\sigma_I(1) = 900, \Delta\sigma_Z = 900), (\Delta\sigma_I(1) = -2000, \Delta\sigma_Z = -2000), (\Delta\sigma_I(1) = 500, \Delta\sigma_Z = 500)$

Initially, the effective and actual stresses are same till it reaches elastic domain for uniaxial. In this biaxial tensile unloading/ compressive loading occurs but compressive never occurs. Fig 9. shows evolution of damage surface and physical occurrence of loading & unloading.

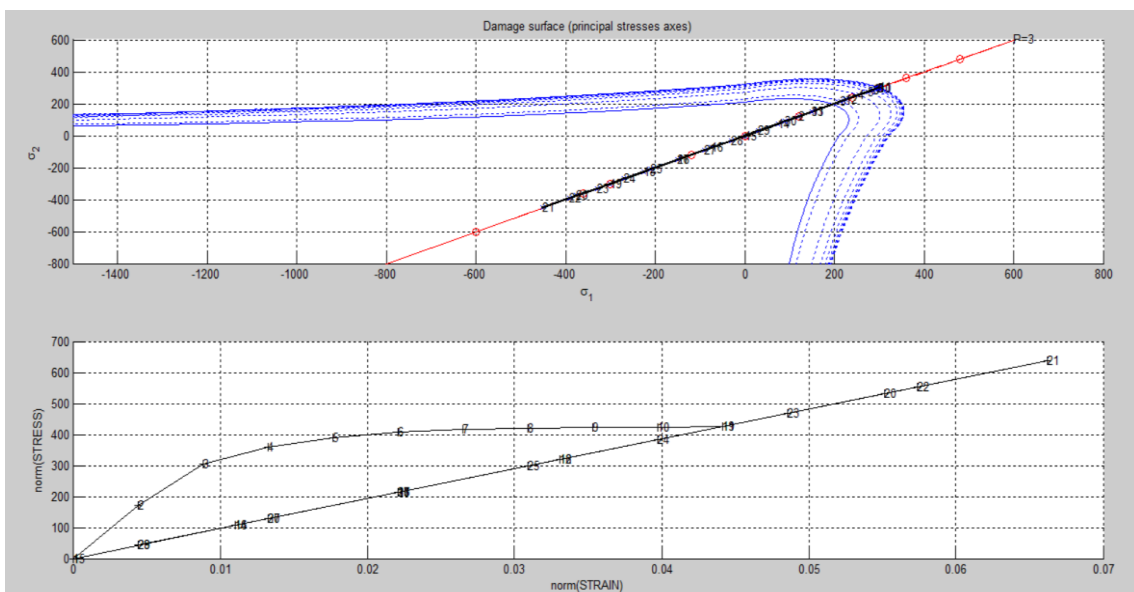


Fig 9: Stress Space & Stress-Strain Curve for the Tensile Damage model

B) Rate Dependent Model

1. Viscous Damage Model

The integration algorithm for viscous damage model for symmetric is implemented. The rate effects are taken into consideration that means evolution of stress depends on strain as well as rate of the strain. The effective stress path is chosen such that $(\Delta\sigma_I(1) = 300, \Delta\sigma_Z = 0)$, $(\Delta\sigma_I(1) = 600, \Delta\sigma_Z = 0)$, $(\Delta\sigma_I(1) = 50, \Delta\sigma_Z = 0)$ and other parameters $\alpha = 0.5$ & $\eta = 0.3$. Fig 10 shows the evolution of actual stresses (stress path) and stress-strain curve for viscous damage model.

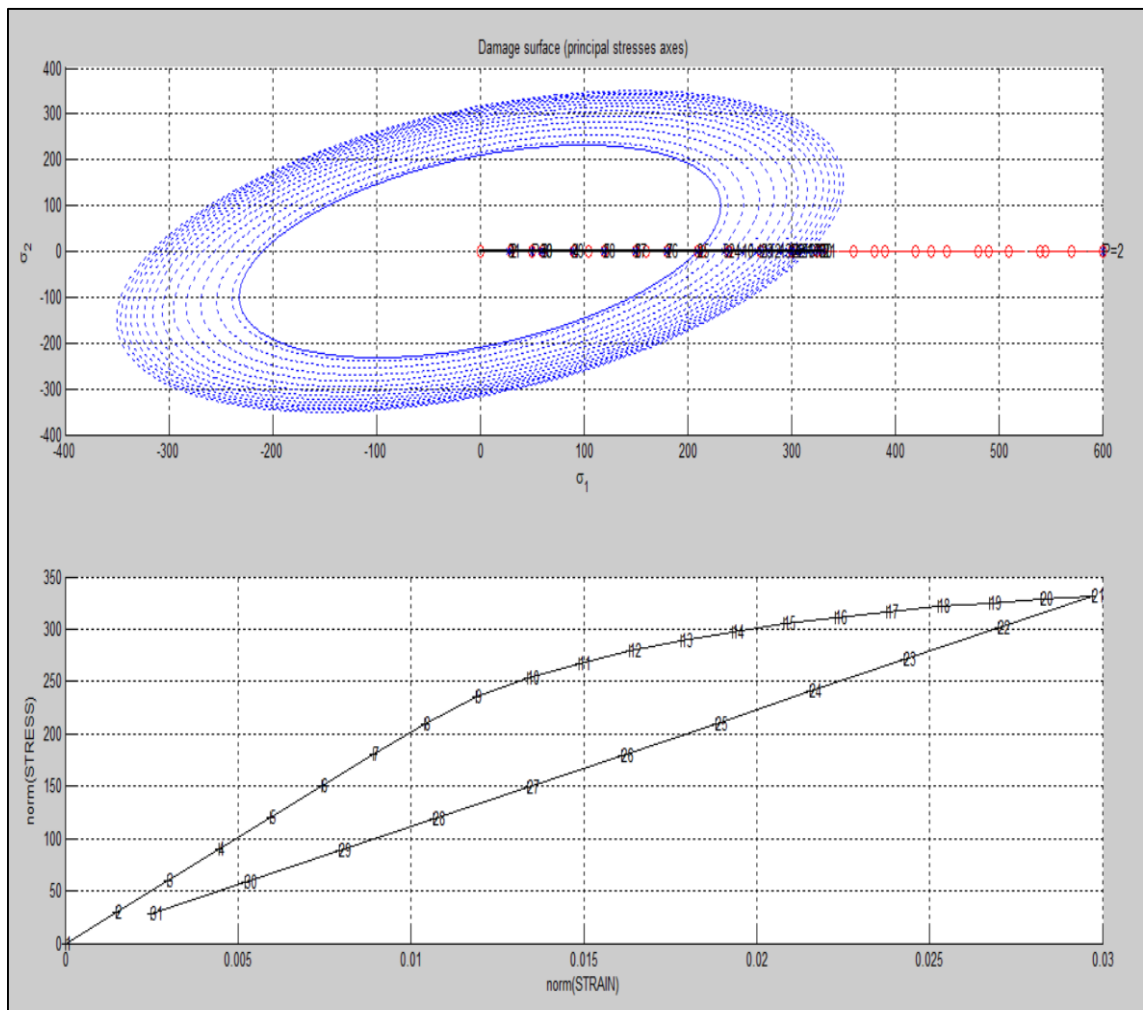


Fig 10: Evolution of actual stresses & Stress-Strain Curve

1.1. Viscosity Variation (ETA)

Outside the elastic region with increase in viscosity, the stress value increase at a definite strain value. Inside the elastic region, stress is independent of viscosity. The stress behaviour is plotted in stress-strain curve for different values of viscosity (η -eta) such as 0, 0.3, 0.5, 0.8 and 1. The effective stress path is $(\Delta\sigma_I(1) = 300, \Delta\sigma_Z = 0)$, $(\Delta\sigma_I(1) = 400, \Delta\sigma_Z = 0)$, $(\Delta\sigma_I(1) = 600, \Delta\sigma_Z = 0)$.

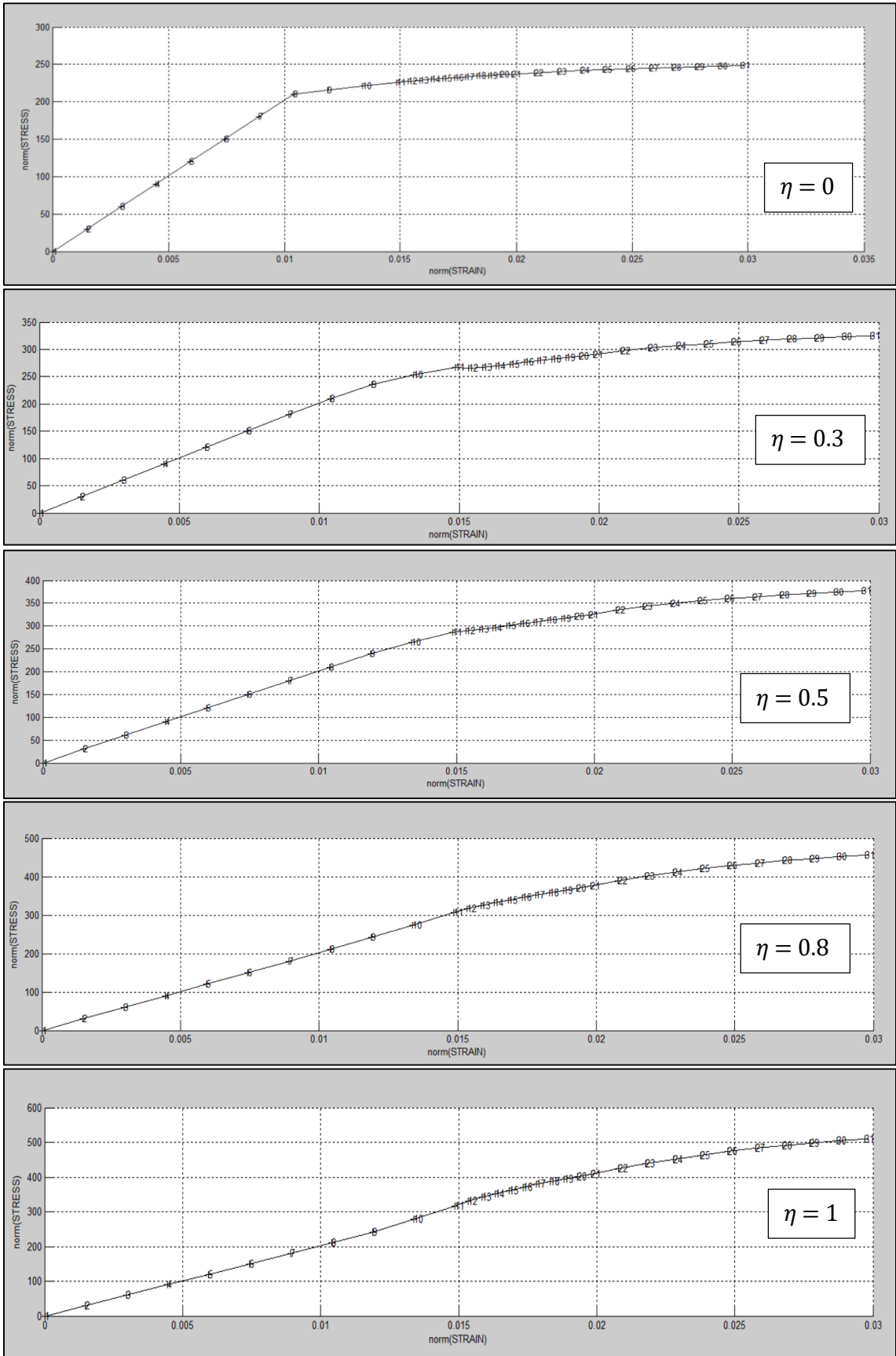


Fig 11: Stress-Strain Curve for Different η

1.2. Strain Rate

Outside the elastic region, increase in the strain rate at particular strain, the value of stress increases. Inside the elastic region, stresses are independent of strain rates. The behaviour of strain rate is plotted in stress-strain curve for different values of strain rate such as 5, 10, 25, 40 and 50. The effective stress path is $(\Delta\sigma I (1) = 300, \Delta\sigma Z = 0)$, $(\Delta\sigma I (1) = 400, \Delta\sigma Z = 0)$, $(\Delta\sigma I (1) = 600, \Delta\sigma Z = 0)$.

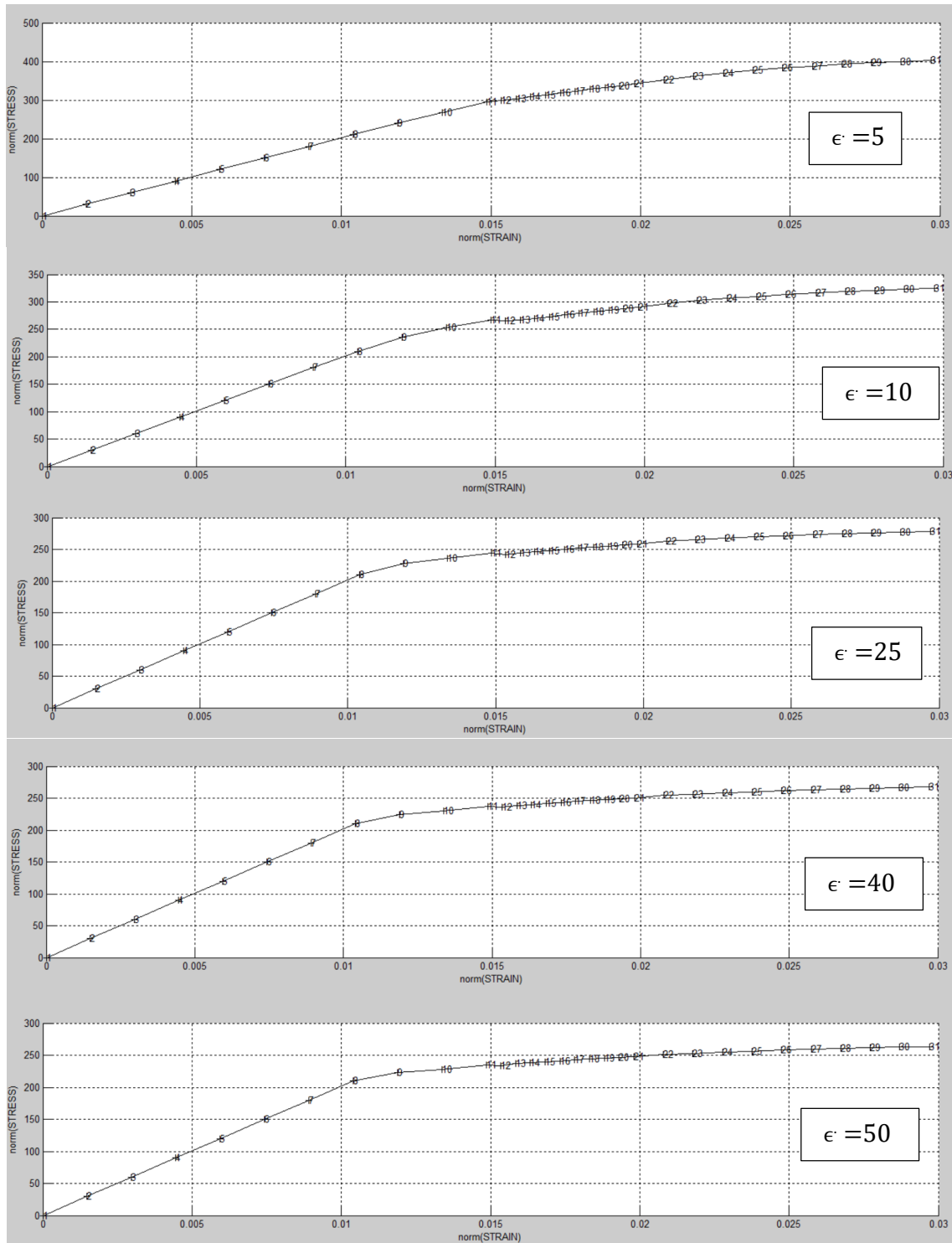


Fig 12: Stress-Strain Curve for Different Strain rates

1.3. Integration Constant (Alpha α)

The effective stress path is $(\Delta\sigma_I(1) = 300, \Delta\sigma_Z = 0)$, $(\Delta\sigma_I(1) = 400, \Delta\sigma_Z = 0)$, $(\Delta\sigma_I(1) = 600, \Delta\sigma_Z = 0)$. It is observed that for $\alpha=0$ the numerical integration scheme is conditionally stable, and this explicit method gives first order accuracy. With the bigger time step size, this scheme becomes unstable. The similar effects are also observed for $\alpha = 0.25$. It is an explicit scheme and gives first order accuracy and it is conditionally stable. For $\alpha= 0.5$, the numerical scheme becomes unconditionally stable and it gives second order accuracy. For $\alpha= 0.75$, the numerical scheme is unconditionally stable and it gives first order accuracy. For $\alpha= 1$, the numerical scheme is unconditionally stable and it gives first order accuracy. It is an implicit scheme.

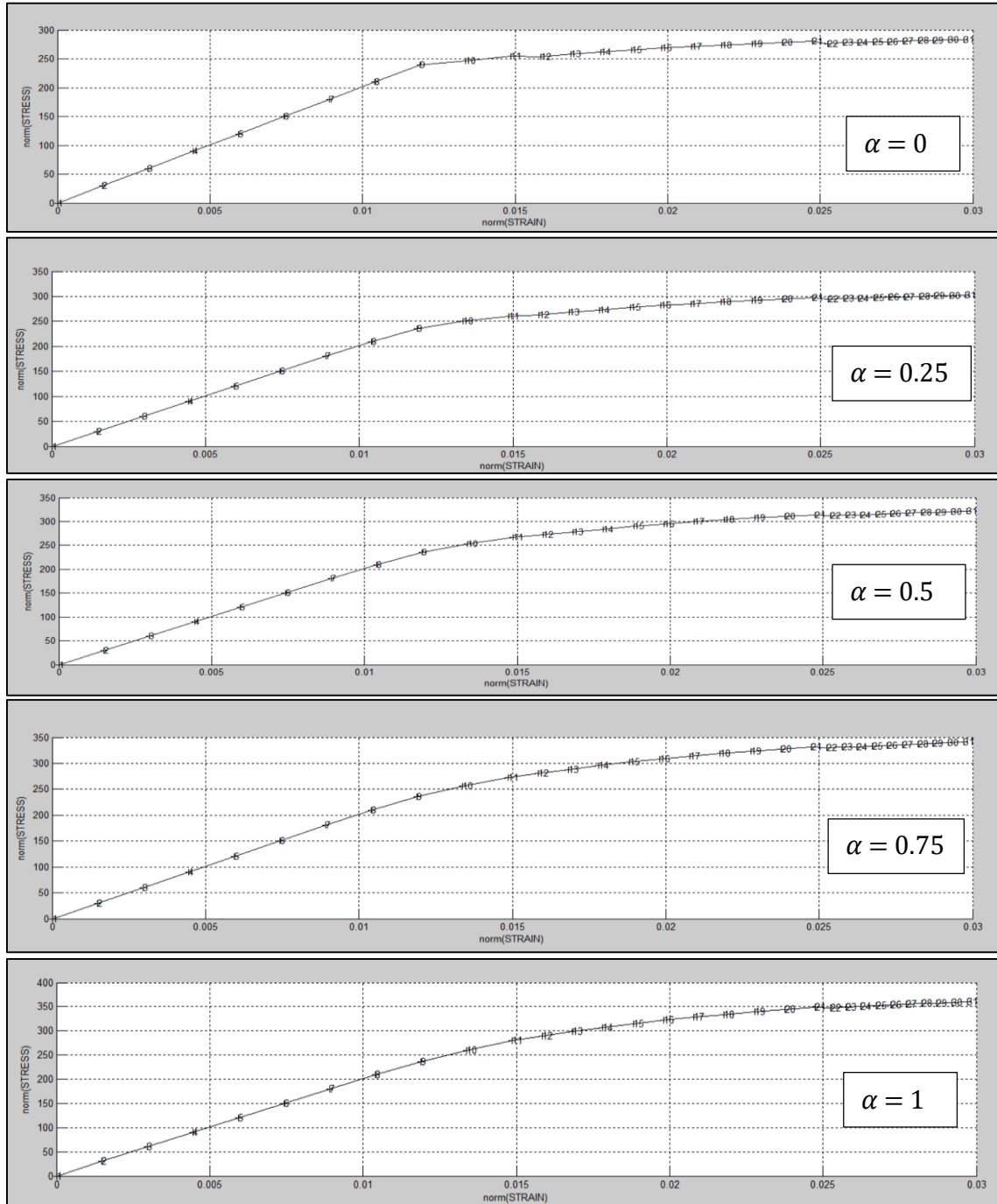


Fig 13: Stress-Strain Curve for Different Integration Constant (Alpha)

2. **Effect of α on the evolution of the along time of the C11 component of the tangent and algorithmic constitutive operators:**

The evolution of the C11 component of the tangent and algorithmic constitutive operators along the time has been studied for the different values of the ' α '. The considered effective stress path, $(\Delta\sigma\bar{\Gamma}(1) = 300, \Delta\sigma\bar{Z} = 0)$, $(\Delta\sigma\bar{\Gamma}(1) = 400, \Delta\sigma\bar{Z} = 0)$, $(\Delta\sigma\bar{\Gamma}(1) = 600, \Delta\sigma\bar{Z} = 0)$. It is investigated that in the elastic domain no evolution takes place for the C11 component of both the tangent and algorithmic constitutive operators along the time. Outside the elastic domain it is found that for higher alpha values at a particular time, the values of the C11 component of the tangent and algorithmic constitutive operators' decreases.

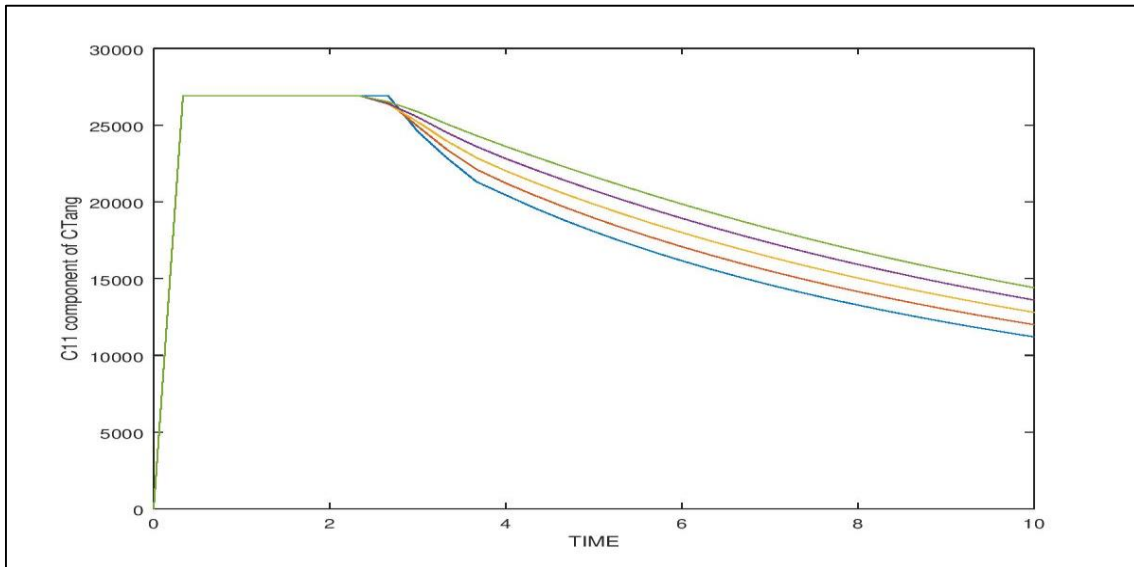


Fig 14: Variation of C11 component of CTang with Time

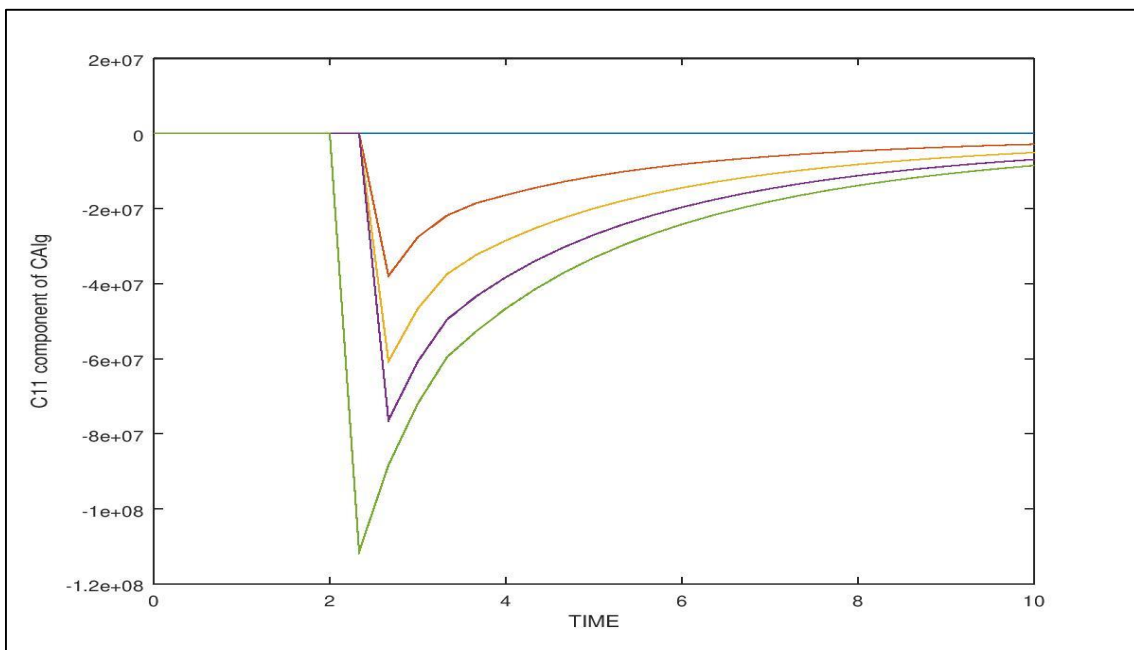


Fig 15: Variation of C11 component of CAlg with Time

Annex (Modified Matlab Codes)

A) Non-Symmetric & Tensile Only Damage Model:

```

%*****
if (MDtype==1)    %* Symmetric

    rtrial= sqrt(eps_n1*ce*eps_n1');

elseif (MDtype==2) %* Only tension

    sigmak=(eps_n1*ce);
    sigmakplus=sigmak.*(sigmak>0);

    rtrial=sqrt(sigmakplus*eps_n1');

elseif (MDtype==3) %* Non-symmetric
    sigmak=(eps_n1*ce);
    sigmaplus=sigmak.*(sigmak>0);
    sigmakabs=abs(sigmak);
    teta=sum(sigmaplus)/sum(sigmakabs);
    C=(teta+(1-teta)/n);

    rtrial= C*sqrt(eps_n1*ce*eps_n1');

end

% POLAR COORDINATES

if MDtype==1 %SYMMETRIC

elseif MDtype==2 %Tensile
    tetha=[(-pi/2)*0.9999:0.01:pi*0.9999];
%*****%* RADIUS
D=size(tetha); %* Range
m1=cos(tetha); %*
m2=sin(tetha); %*
Contador=D(1,2); %*

radio = zeros(1,Contador) ;
s1 = zeros(1,Contador) ;
s2 = zeros(1,Contador) ;

for i=1:Contador
sigma= [m1(i) m2(i) 0 nu*(m1(i)+m2(i))];
sigmaplus=sigma.*(sigma>0);
radio(i)= q/sqrt(sigmaplus*ce_inv*sigma');

s1(i)=radio(i)*m1(i);
s2(i)=radio(i)*m2(i);

```

```

end
hplot =plot(s1,s2,tipo_linea);

elseif MDtype==3  %Non-Symmetric
tetha=[0:0.01:2*pi];
%*****
%* RADIUS
D=size(tetha); %* Range
m1=cos(tetha); %*
m2=sin(tetha); %*
Contador=D(1,2); %*

radio = zeros(1,Contador) ;
s1 = zeros(1,Contador) ;
s2 = zeros(1,Contador) ;

for i=1:Contador
sigma=[m1(i) m2(i) 0 nu*(m1(i)+m2(i))];
sigmaplus=sigma.*(sigma>0);
teta=sum(sigmaplus)/sum(abs(sigma));

radio(i)= (q/sqrt(sigma*ce_inv*sigma'))/(teta+(1-teta)/n);
s1(i)=radio(i)*m1(i);
s2(i)=radio(i)*m2(i);

end

hplot =plot(s1,s2,tipo_linea);
end

%*****

```

B) Exponential Hardening Equation:

```

%*****
if hard_type == 0      %Linear

q_n1= q_n+ H*delta_r;

elseif hard_type == 1  %exponential
%q_inf=r0+r0-zero_q;
q_inf=2;
%q_inf=1e-6*zero_q;
A=1;

H_n= A*(q_inf-r0)/r0*exp(A*(1-r_n/r0));
q_n1= q_n+ H_n*delta_r;
end
end
%*****

```

C) Viscous Model:

```
%*****
%VISCOUS
else
if (rtrial_n_alpha > r_n)
%* Loading
load=1;
delta_r=rtrial_n_alpha-r_n;
% computation of r at the step n+1
r_n1 = (eta - delta_t*(1-alpha))/(eta + alpha*delta_t)*r_n + (delta_t/(eta +
alpha*delta_t))*rtrial_n_alpha;
if hard_type == 0
% Linear
H_n1 = H;
q_n1= q_n+ H_n1*delta_r;
else
H_n= A*(q_inf-r0)/r0*exp(A*(1-r_n/r0));
q_n1= q_n+ H_n*delta_r ;
end
if(q_n1<zero_q)
q_n1=zero_q;
end
else
%* Elastic load/unload
load=0;
r_n1= r_n ;
q_n1= q_n ;
end
end

%*****
```